Theoretical study of β-Ge_3N_4 and its high-pressure spinel γ phase

Jianjun Dong and Otto F. Sankey
Department of Physics and Astronomy, and Materials Research Center, Arizona State University, Tempe, Arizona 85287-1504

Sudip K. Deb, George Wolf, and Paul F. McMillan
Department of Chemistry and Biochemistry, and Materials Research Center, Arizona State University, Tempe, Arizona 85287-1704

(Received 13 December 1999)

We perform a theoretical investigation of the β phase and the high-pressure spinel-like γ phase of Ge_3N_4. The electronic structure is found to yield direct band gaps in the optical region for both phases. The vibration modes and their pressure dependence of β-Ge_3N_4 are determined theoretically, and are compared with experimental Raman spectra. All Raman-active modes are identified and agreement of theory with experiment is excellent. A Raman silent B_u mode of the β phase ($P6_3/m$) is found to become soft under high pressure to yield a reduced symmetry ($P\bar{6}$) β-phase derivative. The β structure changes further to a reduced symmetry $P3$ space group at higher pressure. Theory is used to determine the optimized structural parameters and equations of state (EOS) for all phases, and the EOS yields a theoretical value for the $\beta \rightarrow \gamma$ phase-transition pressure. The vibration modes of the γ phase are determined theoretically and compared to Raman measurements.

I. INTRODUCTION

Group-IV(B) nitrides are an interesting and important class of materials. Silicon nitride (Si_3N_4) is a familiar ceramic material with numerous applications because of its high strength, its resistance to wear, and its desirable high-temperature properties,[1,2] and it has been well studied.[3–9] Si_3N_4 is also used for applications in the microelectronics industry because of its insulating dielectric properties, strength, and as a diffusion mask for impurities. The crystalline form of carbon nitride (C_3N_4) still remains hypothetical,[10–13] but is predicted to be super hard if successfully synthesized in the isostructure of β-Si_3N_4. This material has stimulated intensive research efforts in recent years, and the investigation remains ongoing.

Germanium nitride (Ge_3N_4) is far less studied than its silicon counterpart. The ground-state structure of germanium nitride is isostructural to that of hexagonal β-Si_3N_4.[3] Another phase, trigonal α, is also known to exist both for Si_3N_4 and Ge_3N_4, and its structure is similar to that of β but with a cell doubling and a reduction of symmetry. The α phase transforms into the β phase upon heating, yet the $\beta \rightarrow \alpha$ phase transition is never observed. The corresponding energetics of C_3N_4 is still topic of theoretical investigation.[11–13]

The β phase of Si_3N_4 or Ge_3N_4 consists of corner connected SiN_4 or GeN_4 tetrahedra, respectively. This is not unlike silicon and germanium oxides which contain SiO_4 and GeO_4 linked tetrahedra. The existence of a variety of polymorphs of silicon and germanium oxides hints that other low-energy phases of Ge_3N_4 or Si_3N_4 might exist. Recently, experimental high-pressure studies of Ge_3N_4 have been performed by two groups, and a different crystalline phase (γ-Ge_3N_4) with a cubic unit cell has been successfully synthesized.[14–16] This phase introduces interesting bonding and produces Ge that is octahedrally coordinated. An earlier study produced a similar structure for Si_3N_4.[17]

The experiments of Leinenweber and co-workers[15,16] start with commercial Ge_3N_4 samples, which contains a mixture of α- and β-Ge_3N_4, as well as a small amount of elemental Ge. The sample is purified to β-Ge_3N_4, and subsequently loaded into a diamond-anvil cell (DAC) and pressured up to 40 GPa. The $\beta \rightarrow \gamma$ phase transition occurs near 12–15 GPa. Heating is necessary for the phase transition, which suggests there exists a relatively high-energy barrier inhibiting conversion. At room temperature, the diffraction patterns remain sharp until 15 GPa, and broadens above 19 GPa. A subset of the original (β-phase) diffraction peaks can be followed even up to about 40 GPa. However, with high temperature and high pressure the γ phase appears, which is recoverable to ambient conditions. Rietveld refinement reveals that γ-Ge_3N_4 is the cubic spinel structure ($Fd\bar{3}m$). The synthesis of Ge_3N_4 spinel by Serghiou *et al.*[14] proceeded in the DAC with laser heating using powdered Ge in an N_2 atmosphere, where N_2 acted as the pressure medium and nitrogen source. Heating occurred for several minutes, and temperatures were in excess of 2000 K. In the γ phase, germanium is in both tetrahedral and octahedral coordinations surrounded by nitrogen, and this is a nitride with six-coordinated germanium. The critical phase transition pressure ($\beta \rightarrow \gamma$) is not yet accurately determined. Leinenweber and co-workers reported that pressures greater than 12 GPa are needed at temperatures above 1000 °C.

In this paper, we report a theoretical study of (i) the high-pressure properties of β-Ge_3N_4, and (ii) the high pressure phase γ-Ge_3N_4. We investigate the pressure dependence of the structural and vibrational modes of β-Ge_3N_4, and compare our results with x-ray and Raman-scattering experiments. Our calculations clearly indicate that the near planar Ge_3N units within the β-Ge_3N_4 structure pucker above a calculated pressure of 20 GPa, and the symmetry is lowered from hexagonal $P6_3/m$ to hexagonal $P\bar{6}$. Upon further application of pressure, a second instability occurs near 28 GPa in the calculation, where a second class of NGe_3 units, which initially were exactly planar pucker along the c axis, and the

TABLE I. Structures, symmetries, and internal coordinates of β (hexagonal) and γ (fcc spinel) phases of Ge_3N_4. Four possible space groups are considered for β structure (see discussion in the text). We have added $\frac{1}{4}$ to z in $P\bar{6}$ to emphasize the similarity with the other β derivative structures.

Phase	Space group	Wyckoff site	Site symmetry	Fractional coordinates
β	$P6_3/m$ (C_{6h}^2)	$2c$	$\bar{6}\ldots(C_{3h})$	$(\frac{1}{3},\frac{2}{3},\frac{1}{4})$, $(\frac{2}{3},\frac{1}{3},\frac{3}{4})$
(hexagonal)		$6h$	$m\ldots(C_s)$	$(x,y,\frac{1}{4})$, $(\bar{y},x+\bar{y},\frac{1}{4})$, $(\bar{x}+y,\bar{x},\frac{1}{4})$
				$(\bar{x},\bar{y},\frac{3}{4})$, $(y,\bar{x}+y,\frac{3}{4})$, $(x+\bar{y},x,\frac{3}{4})$
	$P\bar{6}$ (C_{3h})	$1c$	$\bar{6}$	$(\frac{1}{3},\frac{2}{3},\frac{1}{4})$
		$1f$	$\bar{6}$	$(\frac{2}{3},\frac{1}{3},\frac{3}{4})$
		$3j$	m	$(x,y,\frac{1}{4})$, $(\bar{y},x+\bar{y},\frac{1}{4})$, $(\bar{x}+y,\bar{x},\frac{1}{4})$
		$3k$	m	$(x,y,\frac{3}{4})$, $(\bar{y},x+\bar{y},\frac{3}{4})$, $(\bar{x}+y,\bar{x},\frac{3}{4})$
	$P6_3$ (C_6^6)	$2b$	$3\ldots(C_3)$	$(\frac{1}{3},\frac{2}{3},z)$, $(\frac{2}{3},\frac{1}{3},z+\frac{1}{2})$
		$6c$	$1(C_1)$	(x,y,z), $(\bar{y},x+\bar{y},z)$, $(\bar{x}+y,\bar{x},z)$
				$(\bar{x},\bar{y},z+\frac{1}{2})$, $(y,\bar{x}+y,z+\frac{1}{2})$, $(x+\bar{y},x,z+\frac{1}{2})$
	$P3$ (C_3^1)	$1b$	$3\ldots(C_3)$	$(\frac{1}{3},\frac{2}{3},z)$
		$1c$	$3\ldots(C_3)$	$(\frac{2}{3},\frac{1}{3},z)$
		$3d$	$1(C_1)$	(x,y,z), $(\bar{y},x+\bar{y},z)$, $(\bar{x}+y,\bar{x},z)$
γ	$Fd\bar{3}m$ (O_h^7)	$8a$	$\bar{4}3m(T_d)$	$(0,0,0)$, $(\frac{3}{4},\frac{1}{4},\frac{3}{4})$
(cubic)		$16d$	$0.\bar{3}m(D_{3d})$	$(\frac{5}{8},\frac{5}{8},\frac{5}{8})$, $(\frac{3}{8},\frac{7}{8},\frac{1}{8})$, $(\frac{7}{8},\frac{1}{8},\frac{3}{8})$, $(\frac{1}{8},\frac{3}{8},\frac{7}{8})$
		$32e$	$0.3m(C_{3v})$	(x,x,x), $(\bar{x},\bar{x}+\frac{1}{2},\bar{x}+\frac{1}{2})$,
				$(\bar{x}+\frac{1}{2},x+\frac{1}{2},\bar{x})$, $(x+\frac{1}{2},\bar{x},\bar{x}+\frac{1}{2})$
				$(x+\frac{3}{4},x+\frac{1}{4},\bar{x}+\frac{3}{4})$, $(\bar{x}+\frac{1}{4},\bar{x}+\frac{1}{4},\bar{x}+\frac{1}{4})$,
				$(x+\frac{1}{4},\bar{x}+\frac{3}{4},x+\frac{3}{4})$, $(\bar{x}+\frac{3}{4},x+\frac{3}{4},x+\frac{1}{4}$

space group changes to $P3$. These distorted phases are derivatives of the β phase but in the $P\bar{6}$ or $P3$ space groups, and only exist at high pressure if the temperature is insufficient to enable $\beta\rightarrow\gamma$ transformation.

We also report the electronic band structure of the germanium nitride phases and find that both β- and γ-Ge_3N_4 are *wide, direct-gap* semiconductors at zero pressure, which indicates germanium nitride may be promising optoelectronic materials, possibly competitive with group-III(B) nitrides (GaN/InN/AlN).

The calculations in this study are performed using a first-principles total-energy method. The implementation we adopt[18] uses density-functional theory (DFT) with a plane-wave basis set and an ultrasoft pseudopotential.[19] The exchange-correlation functional is approximated with the local-density approximation (LDA) Ceperley-Alder function,[20] or with a generalized gradient approximation (GGA).[21]

II. GEOMETRICAL STRUCTURES, ELECTRONIC STRUCTURE, AND ENERGETICS

A. Optimized structures and equations of state

The two ambient pressure crystalline structures of Ge_3N_4 are the trigonal α structure and the hexagonal β structure. The high-pressure spinel phase of Ge_3N_4 is the γ phase. In this paper we will focus on the β and γ phases. The space groups, symmetries, and internal coordinates for β and γ phases are listed in Tables I and II. In this study, we assume

TABLE II. The optimized lattice parameters and internal coordinates of β- and γ-Ge_3N_4 calculated with LDA methods. The experimental data are from Refs. 3, 15, and 16.

Phase	Lattice Theory	Const Expt	Internal Coordinates Theory	Expt
β	$a=7.987$	8.028	Ge^1 at $6h$: (0.1696,0.7628,1/4)	(0.1712,0.7658,1/4)
$P6_3/m$	$c=3.054$	3.077	N^{6h} at $6h$: (0.3304,0.0257,1/4)	(0.3335,0.0295,1/4)
			N^{2c} at $2c$: (1/3,2/3,1/4)	
γ	$a=8.1676$	8.2133	Ge^1 at $8a$ (Ge^{IV}): (0,0,0)	
$Fd\bar{3}m$			Ge^2 at $16d$ (Ge^{VI}): (5/8,5/8,5/8)	
			N at $32e$: (0.1330,0.1330,0.1330)	(0.1327,0.1327,0.1327)

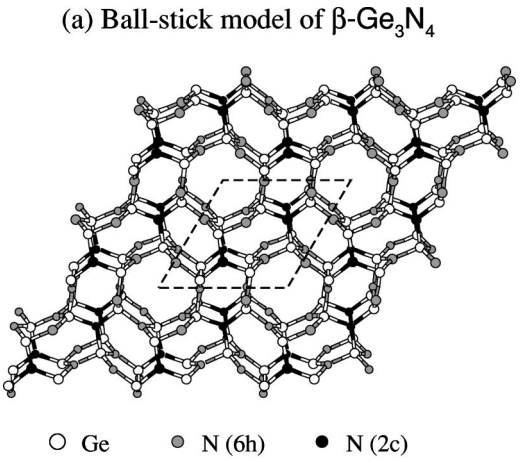

FIG. 1. (a) A ball-stick model of β phase of Ge_3N_4. The dark, light, and open circles represent Ge atoms at $2c$ sites, Ge atoms at $6h$ sites, and N atoms, respectively, of space group $P6_3/m$. (b) A unit cell of β-Ge_3N_4 showing the linking of the GeN_4 tetrahedra.

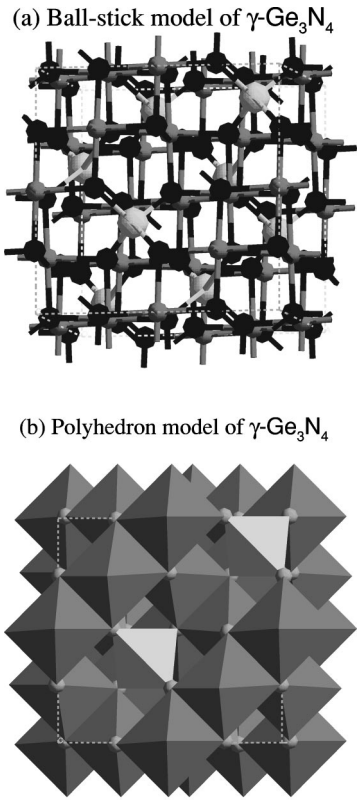

FIG. 2. (a) A ball-stick model of γ phase of Ge_3N_4. The large light spheres are the tetrahedral Ge atoms. (b) A unit cell of γ-Ge_3N_4 showing the linking of the GeN_4 tetrahedra and GeN_6 octahedra.

β-Ge_3N_4 is isostructural to β-Si_3N_4 and that this phase is the ground state of germanium nitride.

The x-ray-diffraction data of β-Ge_3N_4 at ambient condition fit very well with the centrosymmetric $P6_3/m$ space group.[3,15] Within this symmetry, all germanium atoms are four-coordinated at the center of a distorted tetrahedron surrounded by nitrogen, and all nitrogen atoms are three coordinated. The structure is that of phenacite (Be_2SiO_4), and the hexagonal unit cell contains two formula units (14 atoms). Figure 1(a) shows a ball-stick model of β-Ge_3N_4, with its structure being characterized by open 8-atom and 12-atom rings. Unless specifically noted, we will always use the $P6_3/m$ space group for the β-Ge_3N_4 phase. All Ge atoms are equivalent ($6h$ sites), but there are two inequivalent nitrogen sites: N^{2c} at $2c$ sites and N^{6h} at $6h$ sites. The N^{2c} atoms are in a planar geometry with their three Ge nearest neighbors, while the N^{6h} atoms are in slightly puckered sites surrounded by three Ge atoms. There are three less symmetric structures easily derived from the $P6_3/m$ structure—these structures have space groups $P\bar{6}$, $P6_3$, and $P3$ (Tables I and II). Our calculations show (see below) that the $P\bar{6}$ and $P3$ structures occur at high pressure for material not transformed to the γ phase.

The local bonding environment in α- and β-Ge_3N_4 are very similar. The α-Ge_3N_4 is less symmetric than β phase and has the (trigonal) $P31c$ space group. Since trigonal unit cells have equivalent hexagonal cells, we can view α-Ge_3N_4 as consisting of alternate basal layers of β-Ge_3N_4 and its mirror image. Its c axis is approximately twice that of the β phase, and there are four formula units per hexagonal unit cell. Important differences between α and β phases is that in α *all* N atoms lie out of the plane of its three Ge neighbors, and open rings disappear in the α structure.

The γ-Ge_3N_4 has the spinel structure (Tables I and II). Natural spinel is the mineral $MgAl_2O_4$, which written with formal charges is $Mg^{+2}Al_2^{+3}O_4^{-2}$. The Bravais lattice is face-centered-cubic (fcc) in the space group $Fd\bar{3}m$ with eight $MgAl_2O_4$ units in the conventional cubic cell, and two formula units in the primitive unit cell. The Mg atom is four coordinated and is at the center of an oxygen tetrahedron, and the Al is six coordinated and is at the center of a distorted oxygen octahedron. For Ge_3N_4 in the spinel structure, two Ge (Ge^{IV}, $8a$ site) resides at the nominal Mg site and is tetrahedrally coordinated to nitrogen. The remaining four Ge atoms in the formula unit (Ge^{VI}, $16d$ site) reside at the nominal Al sites and are octahedrally coordinated to nitrogen. The nitrogen atoms are all equivalent ($32e$ site) and have four Ge neighbors, with one being Ge^{IV} and three being Ge^{VI}. The space group for the spinel $Ge^{IV}Ge_2^{VI}N_4$ structure is given in Table I, and a model of the spinel Ge_3N_4 structure is shown in Fig. 2.

We first determine the optimized (minimum energy) structures of the β- and γ-crystalline phases of Ge_3N_4. We begin by fixing the volume of the unit cell, and then relax the lattice parameters (consistent with that volume) and the internal coordinates. This optimization is performed with the

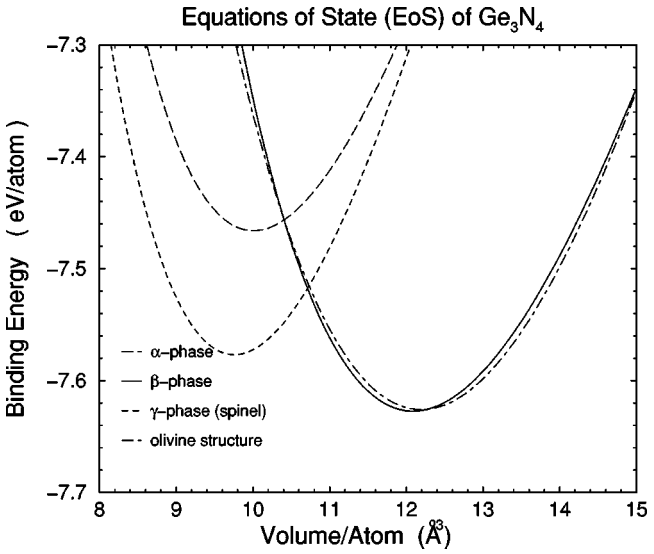

FIG. 3. The calculated equations of state (energy vs volume curves) based on the LDA. The parameters are provided in Table III where they are compared with the GGA. The energy difference between α and β phases is very small (near numerical errors). The γ phase (spinel) is a high-pressure phase of Ge_3N_4, and the energy difference between the γ phase and β phase is 50 meV/atom within LDA (100 meV within GGA). Another high pressure phase is olivine, which lies higher in energy than the spinel phase.

constraint of maintaining the corresponding space-group symmetry. This procedure is repeated for several different unit-cell volumes, and the calculated data are fit to a Birch-Murnaghan energy vs volume equation of state (EOS). There are four parameters in a Birch-Murnaghan EOS; the binding energy E_0, the equilibrium (minimum energy) volume V_0, the bulk modulus K, and the pressure derivative K' of the bulk modulus ($K' = dK/dP$).

The calculated EOS is plotted in Fig. 3, and their parameters are listed in Table III, along with available experimental data.[3,15] For completeness we include the α phase as well. First let us discuss the LDA results. The total-energy difference between α and β phase of Ge_3N_4 is found to be negligibly small at low pressure. Thus either of these two phases can exist at ambient conditions. The γ spinel structure is a higher energy phase that is achievable by the application of pressure. Despite the dramatically different chemical bonding within the β and γ phases, the energy difference between these two phases is only about 50 meV/atom (equivalent to 600 K in temperature units), which is surprisingly small. We have repeated these calculations using the GGA method and find that the major effect of this correction is a fairly rigid shift of 0.9 eV upwards in the total energies. The energy difference between the β and γ phases, however, increases to 100 meV/atom. Since the energy differences found here between these phases is small, the differences should be considered qualitative. In Fig. 3, we also plot the total energy of the olivine structure of Ge_3N_4. This structure is less symmetric than that of spinel, and we find it to be considerably higher in energy than the spinel phase. In isoelectronic oxides, such as Mg_2SiO_4, the olivine structure is the stable phase at room temperature, and transform into spinel at high pressures. This is obviously not the case for nitrides.

Comparing equilibrium volumes with experiment,[3,15,16] the LDA underestimates the equilibrium volume by 1.3, 2.1, and 1.6% for α, β, and γ phases, respectively, while GGA overestimates the volume by 3.1 and 3.7% for β and γ phases, respectively. The consistency is satisfactory, and the percentage errors are typical of *ab initio* DFT methods. LDA and GGA methods underestimate the bulk modulus of β-Ge_3N_4 by about 15 and 24%, respectively, which is a larger error than expected. Both LDA and GGA agree that γ-Ge_3N_4 spinel is stiffer than β-Ge_3N_4 by at least 25% (i.e., the bulk moduli of these two phases differ by over 25%). This increase in stiffness from β to γ is expected based on densification.

The lattice and fractional internal parameters of the equilibrium Ge_3N_4 structures are listed in Table II. The calculated parameters are in good agreement with those of experiment. From these we obtain the bond lengths and bond angles of β and γ phases in Table IV. In β-Ge_3N_4, the

TABLE III. The experimental and theoretical (LDA and GGA) parameters of the Birch-Murnaghan equations of state of the α, β, and γ phases of Ge_3N_4. The α phase is included for completeness. The theoretical data is obtained from a fit of the LDA (GGA) energy vs volume curve. The internal coordinates and lattice parameters were optimized at each volume. The parameter E_0 is the binding energy (minimum energy), V_0 is the optimized (minimum energy) structure volume, K is the bulk modulus, and K' the volume derivative of the bulk modulus. The experimental structural parameters of β and γ (spinel) phases are from Refs. 15 and 16, and those of α phase are from Ref. 3.

Phase		E_0 (eV/atom)	V_0 ($Å^3$/atom)	K (GPa)	K'
α	Experiment (Ref 3)		12.321		
	Theory-LDA	−7.626	12.165	178	2.1
β	Experiment (Ref. 15)		12.308	218	4.0
($P6_3/m$)	Theory-LDA	−7.627	12.053	185	3.7
	Theory-GGA	−6.771	12.685	166	3.7
γ	Experiment (Ref. 15)		9.891	296	4.0
	Theory-LDA	−7.577	9.730	240	4.5
	Theory-GGA	−6.661	10.259	208	4.4

TABLE IV. Bond lengths and bond angles of β-phase and γ-phase Ge_3N_4.

Phase	Atom	Bond length (Å)	Bond angle (°)
β	Ge	1.818($\times$1,Ge-N^{2c})	104.1($\times$1,N^{2c}-Ge-N^{2c})
		1.823($\times$2,Ge-N^{6h})	108.4($\times$2,N^{6h}-Ge-N^{6h})
		1.834($\times$1,Ge-N^{6h})	113.8($\times$1,N^{6h}-Ge-N^{6h})
			110.8($\times$2,N^{2c}-Ge-N^{6h})
	N_{2c}	1.818($\times$3,N^{2c}-Ge)	120.0($\times$3,Ge-N^{2c}-Ge)
	N_{6h}	1.823($\times$2,N^{6h}-Ge)	113.8($\times$1,Ge-N^{6h}-Ge)
		1.834($\times$1,N^{6h}-Ge)	123.0($\times$2,Ge-N^{6h}-Ge)
γ	Ge^{IV}	1.881($\times$4,Ge^{IV}-N)	109.5($\times$6,N-Ge^{IV}-N)
	Ge^{VI}	1.979($\times$6,Ge^{VI}-N)	86.2($\times$6,N-Ge^{IV}-N)
			93.8($\times$6,N-Ge^{IV}-N)
			179.9($\times$3,N-Ge^{IV}-N)
	N	1.881($\times$1,N-Ge^{IV})	112.6($\times$3,Ge^{IV}-N-Ge^{VI})
		1.979($\times$3,N-Ge^{IV})	93.7($\times$3,Ge^{VI}-N-Ge^{VI})

tetrahedron is slightly irregular with N-Ge-N bond angles of 104–111° (ideal 109.5°), and Ge-N bond lengths of 1.181–1.834 Å. The $N^{2c}Ge_3$ is planar, and its three Ge-N-Ge bond angles (intertetrahedron angles) are 120°. However, $N^{6h}Ge_3$ is slightly asymmetric and puckered, with two $\theta_{Ge-N-Ge}$ angles of 123.0° and one at 113.8°. In the high-pressure γ phase, the Ge^{IV} atom is perfectly tetrahedral with bond lengths increased from those of β phase (1.81–1.83 Å) to 1.881 Å. The Ge^{VI} atoms are at the center of a slightly distorted GeN_6 octahedron, with much longer Ge-N bond lengths of 1.979 Å. All the N atoms are four coordinated, but the NGe_4 ''tetrahedron'' is quite irregular.

B. Electronic structure

The LDA electronic band structure of the (hexagonal) β and (cubic spinel) γ phases of Ge_3N_4 is shown in Figs. 4(a) and 4(b), respectively. The top of the valence band is defined to be at zero energy. The bands are generated using pseudopotentials which include the $2s$ and $2p$ valence electrons of nitrogen and the $4s$ and $4p$ valence electrons of germanium. The LDA is known to have significant errors in calculating band gaps; after we discuss the LDA results, we describe approximate corrections using a generalized density-functional theory (GDFT) and obtain corrected estimates of the band gaps.

For the hexagonal β phase [Fig. 4(a)], we see a direct band gap between valence and conduction bands of 2.45 eV at the Γ point ($\vec{k}=000$). The valence bands are segregated into two regions, with 24 states in the upper set of bands and 8 states in the lower energy set. The minimum energy separation in energy between these two sets is 3.55 eV. The lower energy valence set is 4.1 eV wide, and are derived mainly from the eight nitrogen s states. We can compare this band structure to that of β-Si_3N_4, which has been more extensively studied both theoretically[7,8] and experimentally.[22,23] We find that the band structure of β-Ge_3N_4 is quite similar to that of β-Si_3N_4 (not shown), except for one significant difference. The top of valence bands in β-Si_3N_4 is along the Γ-A line with the maximum value about 0.3 eV higher than that of the Γ point. Thus β-Si_3N_4 is indirect, while β-Ge_3N_4 is direct.

The band structure of the γ phase (spinel) Ge_3N_4 is shown in Fig. 4(b). The minimum of the conduction and the maximum of the valence band is found to occur at the Γ point. This produces a direct band gap with a band gap of 2.17 eV. It is somewhat surprising that this material, even with Ge being six coordinated, remains semiconducting, and appears to have a large band gap.

The valence band structure of the γ phase is broader than in the β phase by approximately 0.5 eV overall. This overall broadening and the broadening of the individual set of bands is consistent with an increase in coordination of the atoms. The site-projected partial density of states (DOS) is shown in Figs. 5(a)–(c), which gives an orbital s, p, and d decomposition of the DOS. There is no unique way to perform this decomposition, and the results should be interpreted as qualitative. Clearly s states from nitrogen [Fig. 5(c)] dominates in the low-energy set of bands from -18.3 to -12.7 eV, although there is substantial s-state mixing from the octahedral-site Ge^{VI} [Fig. 5(b)] and the tetrahedral-site Ge^{IV} [Fig. 5(a)]. The upper set of bands from -11 to 0 eV is dominated by nitrogen p states, but hybridization occurs with Ge s and p. At the valence band top, we also see a sharp d-character region mainly from the octahedral-site Ge.

The local-density approximation of DFT is well known to have difficulty predicting band gaps quantitatively. The LDA gives band gaps of 2.45 and 2.17 eV for β and γ phases, respectively. The experimental gap of the β phase remains somewhat uncertain but has been reported to be near 4.5 eV.[24] The γ-phase band gap has not yet been experimentally determined. The approximate 2-eV β-phase band-gap error is about twice that found for Si_3N_4 where we find a 4.26-eV

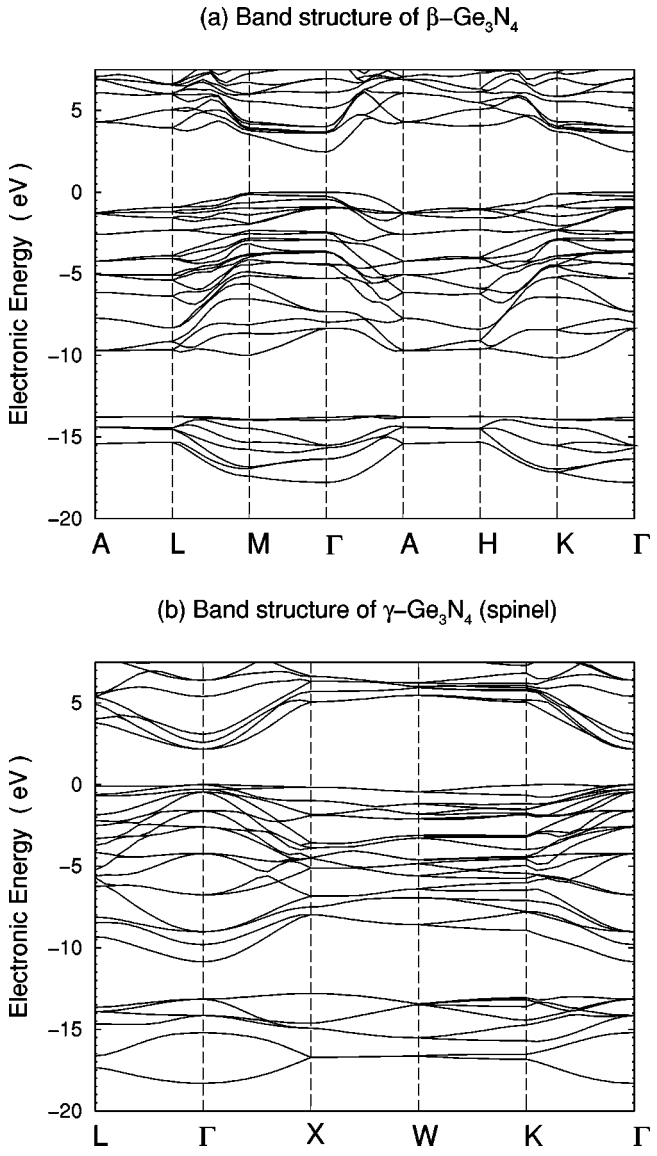

FIG. 4. The LDA electronic band structure of (a) β-Ge_3N_4, (b) γ-Ge_3N_4. A direct wide band gap at the Γ point is found in both phases. For the hexagonal β-Ge_3N_4 (a), the k points correspond to: $A=(0,0,a/2c)$, $L=(1/\sqrt{3},0,a/2c)$, $M=(1/\sqrt{3},0,0)$, $\Gamma=(0,0,0)$, $H=(1/\sqrt{3},1/3,a/2c)$, and $K=(1/\sqrt{3},1/3,0)$ in units of $2\pi/a$. For the cubic spinel phase (b), the k points correspond to: $L=(\frac{1}{2},\frac{1}{2},\frac{1}{2})$, $\Gamma=(0,0,0)$, $X=(\frac{1}{2},0,0)$, $W=(\frac{1}{2},1,0)$, and $K=(\frac{3}{4},\frac{3}{4},0)$ in units of $2\pi/a$. The valence band top is defined to have energy 0.0 eV.

(LDA) gap, while experiments find the band gap to lie in the range of 4.6–5.3 eV.[23] We have tested the GGA for the β phase and find a band gap of 2.48 eV. This result is almost identical to the LDA result of 2.45 eV.

To obtain an improved estimate of the band gap, we have used a generalized density-functional theory (GDFT) to correct the band gaps of the β and γ phases. This theory, which has been developed by Fritsche and co-workers,[25,26] has different levels of approximation, and these levels of approximation have different levels of difficulty. We choose the first level of approximation which gives a band-gap correction of[25]

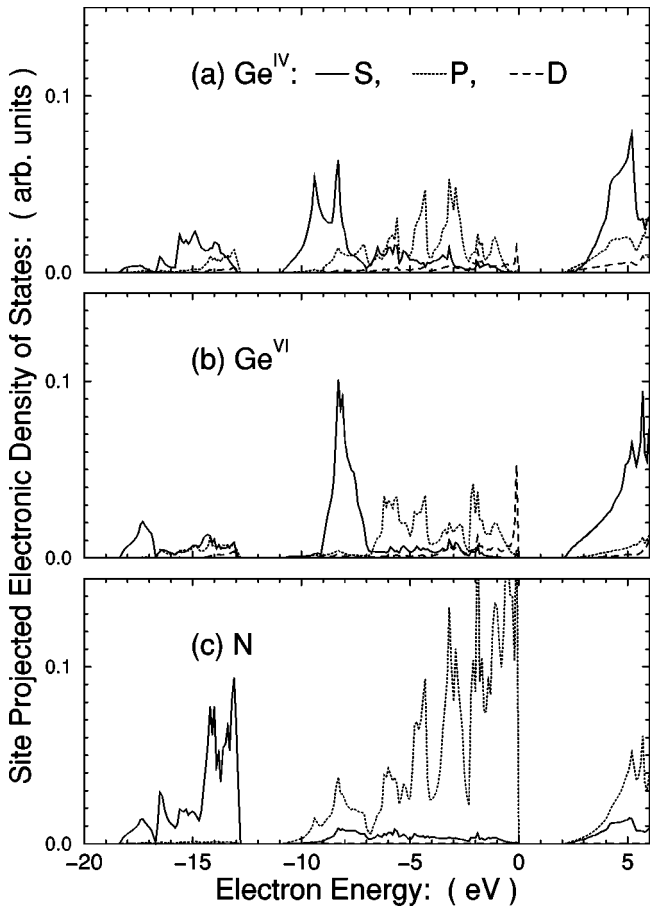

FIG. 5. The site-projected partial electronic density of states of γ-Ge_3N_4 at (a) the Ge^{IV} site, (b) the Ge^{VI} site, and (c) the N site. The solid, dotted, and dashed lines represent *s*-orbital, *p*-orbital, and *d*-orbital decompositions, respectively. The valence bands are those below 0.0 eV.

$$\Delta_{cv}=\int \{2\epsilon_{xc}[n_0(\vec{r})]-\mu_{xc}[n_0(\vec{r})]\} \times[|\psi_c(\vec{r})|^2-|\psi_v(\vec{r})|^2]d^3r, \quad (1)$$

where Δ_{cv} is the correction to be added to the gap separating the conduction (c) and valence (v) electron states (ψ_c and ψ_v, respectively), and ϵ_{xc} and μ_{xc} are the exchange/correlation energy and potentials, respectively, that are used in the LDA. The physics of this approximation is that the total-energy difference between a system with an electron-hole pair and the ground state is not given just by a difference of electron energy eigenvalues, but one must compute the complete total energy which includes the full change in charge density δn [$\delta n(\vec{r})=|\psi_c(\vec{r})|^2-|\psi_v(\vec{r})|^2$]. A further approximation is involved which is that the electron-electron correlation function $f(\vec{r'},\vec{r})$ is unaltered in the excited state containing the electron and hole. The veracity of this approximation is central to the success of Eq. (1).

Fritsche and Gu[25] have evaluated this correction in wide band-gap rare-gas solids, in diamond C and Si, and in alkali halides, while more recently Remediaki and Kaxiras[27] have done a survey of 17 simple zinc-blende (or diamond) semiconductor systems. The results of these two studies show remarkable success. Band-gap errors, which generally were

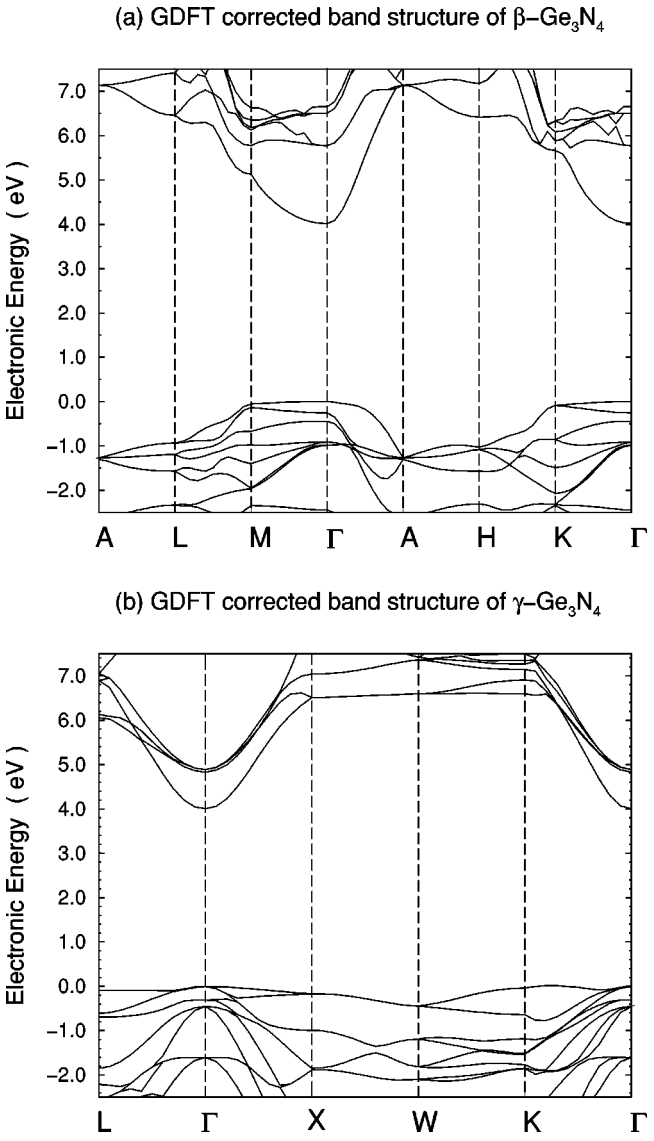

FIG. 6. The GDFT corrected near band-gap electronic structure of (a) β-Ge_3N_4, and (b) γ-Ge_3N_4. The correction is obtained by assuming a hole at the valence-band maximum. The GDFT opens the gaps compared to the LDA results (Fig. 4), and the γ-phase conduction states have been reordered compared to the LDA.

50–100% in LDA, are typically reduced to 10–20% or less in GDFT. These findings, coupled with the fact that the evaluation of Eq. (1) is not computationally difficult (compared to GW or similar methods), makes this an attractive method to correct the gap for the current, more complex, system.

We show the GDFT corrected band structures near the band gap in Figs. 6(a) and 6(b) for β- and γ-Ge_3N_4, respectively. In these figures, we correct the conduction-band states by considering the hole $[|\psi_v|^2$ in Eq. (1)] to be located at the valence-band maximum. We again find direct gaps in both phases, and the band gaps are approximately 4.0 eV in both (coincidentally) β and γ phases. Not unexpectedly, the GDFT opens the gaps, and the opening is approximately 1.5 eV (β) and 1.8 eV (γ). A remarkable result, however, is found for the γ phase. When we compare the GDFT bands [Fig. 6(b)] with the LDA bands [Fig. 4(b)], we find that there has been a significant reordering of the conduction levels. The LDA bands had a triply degenerate conduction-band minimum (p like), while the GDFT bands have a singly degenerate (s like) minimum. Thus in the final GDFT band structure, the valence/conduction transition is now $p \rightarrow s$. This band structure predicts a band-gap optical transition in the UV region of the spectrum, similar to the behavior of the optoelectronic material GaN.

The two approximations, LDA and GDFT, give different conclusions concerning the optical properties of this material. Previous calculations[25,27] for simple structures have shown that the GDFT gives better agreement with experiment for the band gap than the LDA. However, for the more complex spinel structure there is no guarantee that the improvements offered by the GDFT will continue. Furthermore, a reordering of levels as observed here is unprecedented. Ultimately, comparison with experiment will be the final judge as to which approximation offers the best band structure. Experiments are in progress to determine the band gap and optical properties of γ-Ge_3N_4.[28]

C. Phase transition and symmetry reduction at high pressure

The energy difference between the β phase and γ phase (spinel) is relatively small (≈ 0.05 eV/atom in the LDA, and 0.10 eV/atom in the GGA), and hence one would expect that the application of a relatively small pressure would drive a phase transition. We have computed the enthalpy, $H=E+pV$, as a function of pressure for these two phases to obtain an estimate of the equilibrium phase-transition pressure. This analysis neglects entropy differences (assumed to be small) between the two phases. The enthalpies of the two phases are equal at a pressure of 3.7 GPa within the LDA. The phase transition is accompanied by an approximate 2-$Å^3$/atom volume change, or nearly 20%. Similar calculations using the GGA predict a higher phase transition pressure of 7.4 GPa. Experimentally, the phase transition is observed to occur in the same pressure range. Complete transformation to the spinel phase occurs on heating to 1000 °C at 12 GPa,[15] and partial reaction occurs on a laboratory time scale at 10 GPa. However, the transition could not be observed at 9 GPa.

Our calculations also indicate that a metastable transition to an olivine structured phase could occur at higher pressure (13.4 GPa within the LDA), if the $\beta \rightarrow \gamma$ transition could be bypassed. This could be achieved by exploiting the slow kinetics of the reconstructive transformation at low temperature. An olivine phase of a nitride compound has not yet been observed experimentally. In olivine structured oxides such as Mg_2SiO_4 and Ca_2GeO_4, a transition to spinel occurs at high pressure. In Ge_3N_4, the olivine structure lies at higher energy, and any transition would only occur at large negative pressure (Fig. 3).

It is significant that without heating, the $\beta \rightarrow \gamma$ phase transition does not occur. Pressures beyond 20 GPa in the DAC are possible with Ge_3N_4 material remaining in the β phase as evidenced by *in situ* x-ray diffraction. This indicates there exists a large energy barrier for the transformation between the two phases. Beyond 20 GPa, the x-ray pattern becomes significantly broadened, and the β-Ge_3N_4 structure becomes ''softened'' — the volume vs pressure curve bends down-

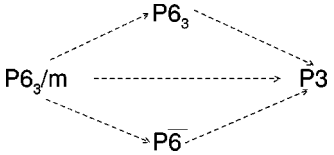

FIG. 7. Three possible paths of symmetry reduction for β-Ge_3N_4 at high pressure. Both $P6_3$ and $P\bar{6}$ are subgroups of $P6_3/m$, and $P3$ is subgroup of $P6_3$ and $P\bar{6}$.

ward (the negative slope becomes steeper).[29] Beyond about 40 GPa, the β-Ge_3N_4 samples become amorphouslike.[15]

We have investigated the metastability of β-Ge_3N_4 at high pressure by examining distortions of the unit cell to less symmetric forms. We begin with the centrosymmetric $P6_3/m$ structure. Two other space groups with relatively lower symmetry, $P6_3$ (Ref. 4) and $P3$,[11] were proposed earlier as possible candidates for the β-Si_3N_4. A mild reduction of symmetry is to the $P\bar{6}$ structure which preserves the mirror planes. The possible paths of symmetry reduction are illustrated in Fig. 7. Table I shows that the relationship amongst these structures is simple. We first investigate structures in which the mirror plane is lost. The high symmetry of $P6_3/m$ is reduced to $P6_3$ by relaxation of $z=\frac{1}{4}$ in the $2c$ and $6h$ sites of $P6_3/m$, to arbitrary z to form the $2b$ and $6c$ sites, respectively, of the $P6_3$ structure. One effect of this is to relax the constraint that N^{2c} is planar in its three-fold coordination to Ge. The symmetry of $P6_3$ can be reduced further to $P3$ by allowing the $2b(P6_3)\rightarrow 1b+1c(P3)$ and $6c(P6_3)\rightarrow 3d+3d(P3)$.

We start with a relaxed structural model of centrosymmetric β-Ge_3N_4 ($P6_3/m$), and reduce the symmetry to $P6_3$ by randomizing the appropriate internal z coordinates from $\frac{1}{4}$ to $\frac{1}{4}+\delta$. Here δ was chosen randomly with an rms displacement of about 0.05 Å. The internal coordinates were allowed to respond to their forces to search for a new energy minimum. The external lattice parameters were held fixed during the search. Three volumes were considered corresponding to pressures of about 10, 30, and 65 GPa based on the EOS of $P6_3/m$ structure of β-Ge_3N_4. (These pressures are likely to be overestimated because of the underestimation of calculated bulk modulus.) In all three simulations, the structural parameters reverted back to $P6_3/m$. Thus we conclude that deviations from $P6_3/m$ to $P6_3$ are not likely in β-Ge_3N_4 even at high pressure.

We performed a similar simulation but reducing the symmetry from $P6_3/m$ to $P3$, where $P3$ is the lowest symmetry space group considered. At zero pressure the atomic positions of the $P3$ structure returned back to those of the $P6_3/m$ space group. However at higher pressure, the $P3$ structure or its $P\bar{6}$ higher symmetry parent structure remained stable and was of lower energy. Figure 8 shows the energy vs volume curves of the $P\bar{6}/P3$ structures along with that of the $P6_3/m$ structure. The energy minimum of $P6_3/m$ is near 12 Å^3/atom. But at a volume of about 11 Å^3, the symmetry changes slowly to $P\bar{6}$ symmetry. This would correspond to a second-order phase transition associated with a soft zone-center mode in our calculations. The coordinate (irreducible representation) that would carry $P6_3/m$ into $P\bar{6}$ would have symmetry B_u (within point group C_{6h}). This

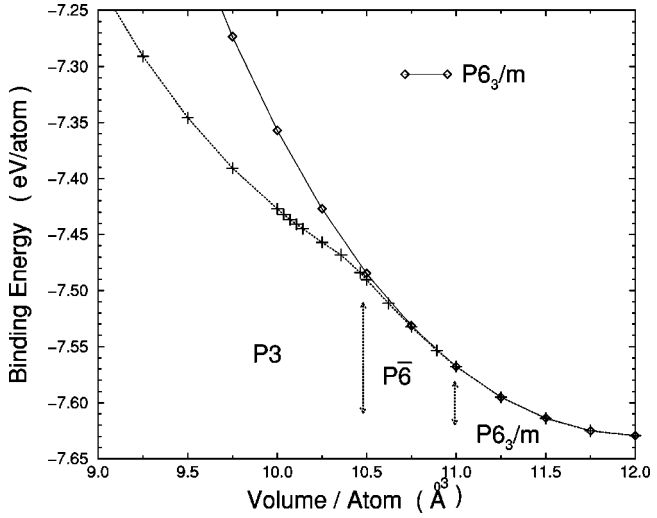

FIG. 8. The total energy of the $P6_3/m$, $P\bar{6}$, and $P3$ structures of β-Ge_3N_4 as a function of volume. The curve for the $P6_3/m$ structure was obtained by enforcing that the structure stay in this symmetry. To calculate the $P6_3/m$-$P\bar{6}$-$P3$ curve, we started with a lowest symmetric $P3$ structure and allowed the atoms to either relax back to $P\bar{6}$ (or $P6_3/m$), or remain in $P3$. There are two structural transitions at 11 Å^3 ($P^*=20$ GPa) and the other near 10.5 Å^3 ($P^{**}=28$ GPa). The first correspond to $P6_3/m\rightarrow P\bar{6}$, and the second to $P\bar{6}\rightarrow P3$.

transformation conserves the mirror plane normal to c axis, but destroys the inversion center. In the $P\bar{6}$ β structure, the nearly planar N atoms pucker while the exactly planar N atoms remain planar. The calculated critical pressure (P^*) of this phase change is about 20 GPa.

As we increase the pressure, a second phase transition is found to occur at a volume near 10.5 Å^3. This transition corresponds to the puckering at the originally perfectly planar N sites, and the mirror plane is lost. The transformation coordinate in this case is of A'' symmetry for the $P\bar{6}$ (C_{3h} point group) (correlated with a B_g or A_u representation within the original $P6_3/m$ space group). The calculated pressure at which this change occurs is P^{**} and is about 28 GPa. Since the $P6_3/m$-$P\bar{6}$-$P3$ EOS curve in Fig. 8 ''bends'' after the second ''puckering'' occurs (between 10.25 and 10.5 Å^3), there exists a common tangent line that links the structure in the $P6_3/m$ space group to the structure in the $P3$ structure. In this sense, it is possible that the $P\bar{6}$ phase is by-passed and the $P6_3/m$ β-Ge_3N_4 transforms into the P3 phase directly via a first-order transition, and the corresponding transition pressure P^{***} is about 23 GPa (a little bit higher than P^*, but lower than P^{**}). Which path is followed depends on the kinetics of the transition. This phase transition would be associated with a large volume decrease (over 10%). This has now been observed in x-ray experiments.[29] We note, however, that these calculations are carried out with the assumption that structural relaxations occur at the Brillouin-zone center, which may not be the case experimentally (see below, and also Ref. 29).

At the current stage, the sequence of phase changes we find for β-Ge_3N_4 are $P6_3/m\rightarrow P\bar{6}\rightarrow P3$. The two structural changes that occur in the system are illustrated in Figs.

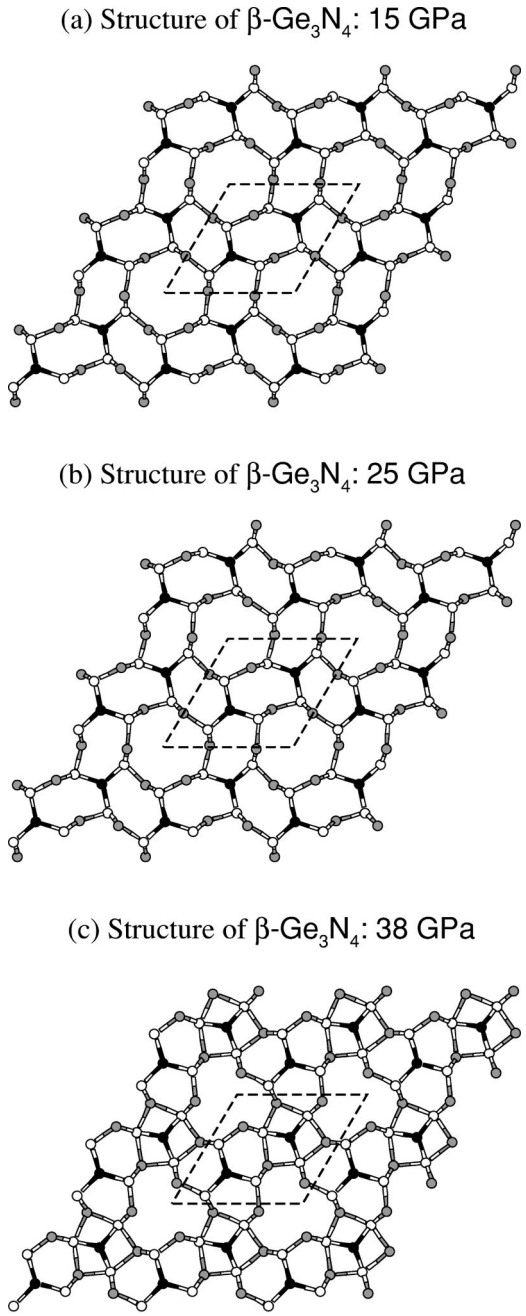

FIG. 9. The structure of β-Ge_3N_4 at three pressures. (a) At 15 GPa in the $P6_3/m$ structure, (b) at 25 GPa which is past the first transition pressure P^* and in the $P\bar{6}$ structure, and (c) at 38 GPa which is past the second transition at P^{**} to $P3$.

9(a)–9(c). Figure 9(a) shows the $P6_3/m$ structure at 15 GPa which is just below the first phase change P^* where the structure changes from $P6_3/m$ to $P\bar{6}$. In Fig. 9(b) at 25 GPa, the structure has changed to $P\bar{6}$. The most significant structural feature is that there is significant motion of the N^{6h} atoms which pucker more significantly away from their three surrounding Ge atoms. This reflects itself as an irregular looking 12-atom ring. [Compare the 12-rings of Fig. 9(a) with Fig. 9(b).] The N^{2c} atoms (of $P6_3/m$) are perfectly planar, and remain so in $P\bar{6}$ past P^* as in Fig. 9(b). As we increase the pressure further passing P^{**}, the atoms rearrange themselves within the unit cell, and transform from $P\bar{6}$ to $P3$ [as shown in Fig. 9(c). Here we see significant distortions, and the planar N^{2c} (of $P6_3/m$) pops out from the Ge_3 plane (although this aspect is not evident in Fig. 9(c)]. There occurs a change in bonding with some N^{6h} atoms (of $P6_3/m$) forming four bonds. Smaller rings (4 and 6 rings) replace some of the 8 and 12 rings. The 3 and 4 bonded nitrogen gives an intermediate hybrid structure between β and γ phases. This phase may contain fivefold coordinated Ge atoms, which is quite unusual for this type of structure.

TABLE V. The theoretical Γ-point $[\vec{q}=(000)]$ vibrational frequencies ω of the hexagonal β ($P6_3/m$) and γ spinel ($Fd\bar{3}m$) phases of Ge_3N_4. Modes are labeled R and IR for Raman and Infrared active, respectively.

β phase ω (cm^{-1})	(hexagonal) Symmetry	γ phase ω (cm^{-1})	(spinel) Symmetry
0	A_u	0	T_{1u}
0	E_{1u}	153	T_{2u}
106	E_{2g} (R)	224	T_{1u} (IR)
108	A_g (R)	245	T_{2g} (R)
129	E_{1g} (R)	245	E_u
137	B_u	406	T_{1u} (IR)
169	E_{2u}	453	T_{1g}
172	B_g	455	A_{2u}
247	A_u (IR)	467	E_g (R)
254	B_g	475	T_{1u} (IR)
271	E_{1u} (IR)	535	T_{2u}
275	E_{2g} (R)	576	T_{2g} (R)
306	B_u	656	T_{1u} (IR)
309	A_g (R)	667	E_u
339	E_{1u} (IR)	710	T_{2g} (R)
365	B_u	806	A_{2u}
373	E_{2g} (R)	830	A_{1g} (R)
443	A_g (R)		
703	A_u (IR)		
721	E_{1g} (R)		
735	E_{2u}		
739	E_{1u} (IR)		
753	B_g		
781	A_g (R)		
791	E_{2g} (R)		
878	E_{1u} (IR)		
878	E_{2g} (R)		
896	B_u		

III. VIBRATIONAL MODES AND RAMAN SPECTRA

In this section, we investigate the vibrational properties of the β and γ phases of Ge_3N_4. We compare the results of theory with those of Raman experiments for both the β and γ phases at zero pressure, and we examine the pressure dependence of the modes for the β phase and compare with experiment. A spectroscopy inactive (''silent'') B_u is found to become soft with pressure in the β phase, which we find leads to a reduction of symmetry from the $P6_3/m$ space group to $P\bar{6}$, consistent with the analysis of Sec. II. At slightly higher pressure, a second mode with A'' symmetry

TABLE VI. Experimental and theoretical Raman shifts of β-Ge_3N_4 at zero pressure. All 11 Raman active modes ($4A_g+2E_{1g}+5E_{2g}$) are found in the experimental spectra.

Symmetry	E_{2g}	A_g	E_{1g}	E_{2g}	A_g	E_{2g}	A_g	E_{1g}	A_g	E_{2g}	E_{2g}
Theory (cm^{-1})	106	108	129	275	309	373	443	721	781	791	878
Expt (cm^{-1})	110	115	131	284	307	377	447	743	798	813	896

(referred to the $P\bar{6}$ phase) leads to the $P3$ phase observed at high pressure.[30]

We theoretically determine the vibrational modes by diagonalizing the force-constant matrix. The force-constant matrix is calculated from the first-principles electronic structure method described earlier, using a direct computational approach.[31,32] In this approach, one begins with the zero-force (minimal energy) structure, and a *single* atom is displaced by a small, yet finite, distance U_0. This calculation produces one complete row of the force-constant matrix. This row is obtained by dividing the forces on each atom by the finite displacement U_0. Point-group symmetry is used to relate rows of the force-constant matrix and only ''independent'' rows are calculated. This theoretical approach produces phonon frequencies and mode displacement patterns which are exact if the system is harmonic. Calculations using both $+U_0$ and $-U_0$ are performed, and the average force-constant matrix produces an error that is fourth order in the displacements.

The Γ point [$\vec{k}=(000)$] phonon mode frequencies are of special interest because they are detected in Raman and infrared (IR) experiments. The Raman and IR spectra act as ''signatures'' to identify the phases, and its pressure dependence reveals information on structural stability and phase transitions. We first present theoretical results for these modes at zero pressure and compare with the experimental Raman spectra for both β and γ phases.

There are 42 Γ-point vibrational modes in β-Ge_3N_4. The centrosymmetric space group ($P6_3/m$) is adopted. The irreducible representations of the Γ-point phonon modes are $\Gamma^{\beta}_{optic}=4A_g+3B_g+2E_{1g}+5E_{2g}+2A_u+4B_u+4E_{1u}+2E_{2u}$ and $\Gamma^{\beta}_{acoustic}=A_u+E_{1u}$. Here 11 modes ($4A_g+2E_{1g}+5E_{2g}$) are Raman active, and 6 modes ($2A_u+4E_{1u}$) are IR active. For reference, if the symmetry of the β phase were reduced to the $P\bar{6}$ or $P3$ space groups, there are 28 Γ-point phonon frequencies which are $8A'(R)+6A''(\mathrm{IR})+10E'(R,\mathrm{IR})+4E''(R)$ (in $P\bar{6}$), and $14A(R,\mathrm{IR})+14E(R,\mathrm{IR})$ (in $P3$). Here, R and IR represent Raman active and IR active, respectively.

A similar factor group analysis of the γ phase (spinel) shows that $\Gamma^{\gamma}_{optic}=A_{1g}+E_g+T_{1g}+3T_{2g}+2A_{2u}+2E_u+4T_{1u}+2T_{2u}$ and $\Gamma^{\gamma}_{acoustic}=T_{1u}$, where five frequencies ($A_{1g}+E_{1g}+3T_{2g}$) are Raman active, and the $4T_{1u}$ modes are IR active.

The calculated Γ-point phonon frequencies of β- and γ-Ge_3N_4 are listed in Table V. These modes are calculated at the minimum-energy geometry for these structures at zero pressure. The frequency range for optic modes in the β phase is about 100–900 cm^{-1}, which is about 100 cm^{-1} wider than that of the γ phase (150–830 cm^{-1}).

A comparison of the measured Raman shifts with those calculated are shown in Tables VI and VII for β and γ phases, respectively. A complete description of the experimental measurements is given in Ref. 33. Experimental Raman results for the spinel phase are also given by Serghiou *et al.*[14] But Deb *et al.*[33] note some potential problems with these measurements. All the possible Raman modes of the γ phase expected by group theory are detected in the experiments. The overall agreement between theory and experiment in both phases is outstanding, with typical discrepancies of 1–3 %. The singular major discrepancy between theory and experiment is the frequency of the lowest T_{2g} mode of the γ spinel phase. Theory predicts it to be at 245 cm^{-1} while the Raman experiment finds 325 cm^{-1}. The origin of this one major discrepancy is unclear.

The pressure dependence of the Γ-point phonon modes provides information about the dynamic stability of the material. Here we investigate the pressure dependence of the modes for the hexagonal β phase. We show the pressure dependence of three types of modes—Raman active modes [Fig. 10(a)], IR active modes [Fig. 10(b)], and silent modes [Fig. 10(c)]. Figure 10(a) also shows the comparison of the pressure dependence of the experimentally measured Raman frequencies and the *ab initio* frequencies. Theory and experiment track each other with pressure extraordinarily well. Overall, Figs. 10(a)–10(c), show that the general behavior of the β-Ge_3N_4 modes can be grouped into three categories. (i) The high-frequency modes (above 700 cm^{-1}) shift upward significantly with pressure at a rate of about 5 cm^{-1} per GPa. (ii) All (except three) low-frequency modes (below 500 cm^{-1}) are relatively insensitive to pressure. The (typically upward) slope of the modes is 1.5 cm^{-1} per GPa or less. Most remain nearly constant over the 20 GPa pressure range. (iii) Three low-frequency mode (the silent B_u mode near 140 cm^{-1}, the silent B_g mode near 170 cm^{-1}, and the IR active A_u mode near 250 cm^{-1}) behave quite differently from the others. These modes become soft with pressure. More interestingly, the B_u mode reaches zero frequency (a dynamically unstable lattice) just under 20 GPa [Fig. 10(c)]. This B_u phonon softening relates to the symmetry reduction of $P6_3/m$ to $P\bar{6}$ found earlier. The critical pressure (about 20 GPa) of this softening is the pressure P^* described in Sec. II, and this pressure may be overestimated in our calculations.

We now analyze this lattice instability in more detail. Atoms in the β-Ge_3N_4 ($P6_3/m$) structure are located in mirror

TABLE VII. Experimental and theoretical Raman shifts of γ-Ge_3N_4 at zero pressure. This structure has five Raman active modes ($1A_{1g}+1E_g+3T_{2g}$).

Symmetry	T_{2g}	E_g	T_{2g}	T_{2g}	A_{1g}
Theory (cm^{-1})	245	467	576	710	830
Expt (cm^{-1})	325	472	593	730	858

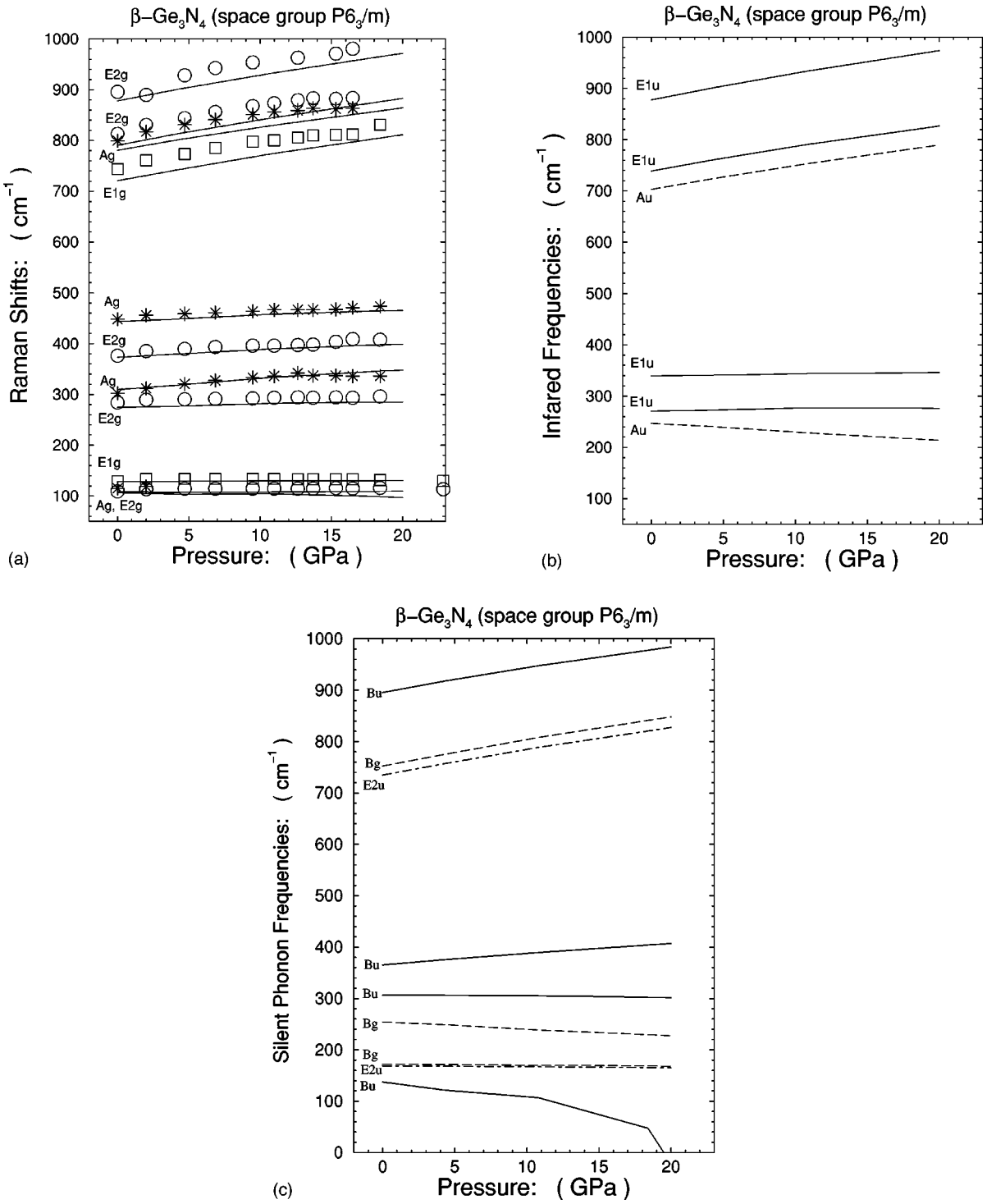

FIG. 10. Phonon modes at $k=(000)$ of (hexagonal) Ge_3N_4. The space group of the β phase in the calculations is taken to be centrosymmetric $P6_3/m$. (a) The calculated (lines) and measured (discrete symbols) pressure dependent Raman shifts of β (hexagonal) Ge_3N_4. The star, square, and circle represent theoretically assigned A_g, E_{1g}, and E_{2g} modes, respectively. (b) The calculated pressure dependence of frequencies of IR active modes. No experimental data of the IR spectra is available. The dotted and solid lines represent A_u and E_{1u} modes, respectively. (c) The ''silent'' (neither Raman or IR active) phonon modes. The solid, dashed, and dash-dotted lines represent B_u, B_g, and E_{2u} modes, respectively. Silent modes behave similar to Raman or IR active modes, except the lowest frequency B_u mode, which goes soft when pressure is applied, leading to an unstable structure.

planes, and the Γ-point phonon modes group into modes with displacements either in the *x,y* plane or along the *z* direction. The A_g, B_u, E_{1u}, and E_{2g} modes have displacement patterns in the *x,y* plane, and the A_u, B_g, E_{2u}, and E_{1g} modes have displacements along *z*. The soft mode is B_u, so this mode displaces atoms in the *x,y* plane. The displacement pattern from the eigenvector of the dynamical matrix shown in Fig. 11 confirms this. The displacement pattern is seen to produce a ''puckering'' of the N^{6h} from a nearly planar configuration, to one that is more pyramidal. As pressure is ap-

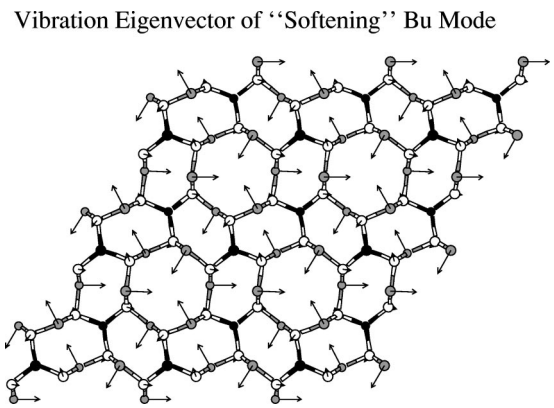

FIG. 11. The vibrational pattern of the B_u soft mode near but below 20 GPa in $P6_3/m\beta$-Ge_3N_4. The open circles are Ge atoms and dark circles are N atoms [also see Fig. 1(a)].

plied, the bonds between N and Ge shorten, until 20 GPa, when the system responds by allowing N^{6h} to become pyramidal. One also notes that the B_{1u} displacement pattern has no z component on the N^{2c} planar atoms. For a finite value of this displacement pattern, the space group changes from $P6_3/m$ to $P\bar{6}$. This reduction in symmetry is entirely consistent with the discussion in Sec. II, but now we have identified the soft phonon driving the first transition. The second transition involves similar atomic displacements, but involving the second set of N atoms away from the sites related by the mirror plane. In a related experimental paper,[30] we have obtained the Raman spectrum of the β-Ge_3N_4 sample above 20 GPa. The spectrum obtained is closely matched by the calculated spectrum of the $P3$ phase, indicating that the second transition has taken place by this (experimental) pressure. However, an additional set of weak peaks is observed in that study, indicating that an incommensurate structure might be present. This indicates that some phonon condensation away from the Brillouin-zone center may take place.[29] Here we examine one possibility that has been previously suggested in the literature.

Mirgorodsky, Baraton, and Quintard[34] have given an elegant analysis of mode softening of β-Si_3N_4, which is very similar to the picture presented here for β-Ge_3N_4. In their work, they were seeking mode softening that might relate to the $\alpha \Leftrightarrow \beta$ transition. Their analysis finds that the two silent modes B_u and B_g [these correspond to the B_u mode near 140 cm^{-1} and the B_9 near 170 cm^{-1} at zero pressure in our work, Fig. 10(c)] couple for $\vec{k}$-dependent phonons along the c axis. Thus their analysis predicts a coupling between x,y motion of the N^{6h} and the planar N^{2c} nitrogen. For $\vec{k}=(\pi/c)(0,0,q)$, with $q=[0,1]$, the $\Gamma \rightarrow \Delta$ compatibility relations show the Δ_2 modes are a combination of B_u+B_g. The significance of this analysis is that the softening can possibly first occur at a q value not equal to zero, producing a phase transition to an incommensurate phase. We note, however, that their results were obtained from force constants obtained by fitting to experiment. At that time, the 144-cm^{-1} A_g mode was misidentified and is now known to be near 450 cm^{-1}.[9] So their model tends to underestimate the low-frequency modes.

To check for a softening at a q value other than zero in β-Ge_3N_4, we have evaluated the pressure dependence of the

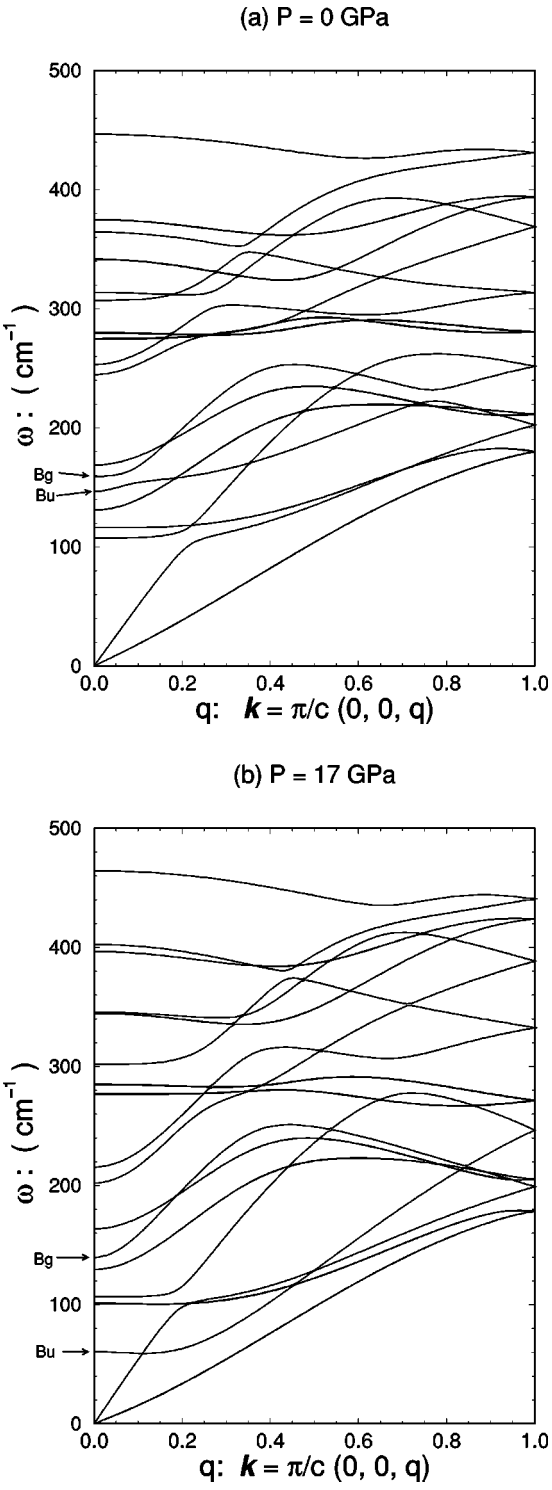

FIG. 12. The phonon dispersion curves for hexagonal β-Ge_3N_4 ($P6_3/m$) for $\vec{k}=(\pi/c)(00q)$ at two pressures. (a) At zero pressure, and (b) at 17 GPa which is slightly below the pressure where the $q=0$ B_u mode goes to zero frequency. No clear softening of modes other than at $q=0$ is evident.

phonon modes with $\vec{k}=(\pi/c)(0,0,q)$. We are searching for q values that might introduce soft modes before the $q=0$ (Γ) point mode. We constructed a supercell of length $5c$ along the z axis, and from this we construct the q-dependent dynamical matrix using force constant between planes up to 7.5 Å apart. The phonon dispersion of the modes at zero

pressure are shown in Fig. 12(a), and at 17 GPa in Fig. 12(b). The 17-GPa results are at a pressure less than 3 GPa away from where the $q=0$ phonon mode goes to zero. The important band in these figures is the band whose Γ-point mode is of B_u symmetry. We see that at 17 GPa, the B_u mode has moved down from its value at zero pressure as expected from Fig. 10(c). This mode moves down with pressure slowly until very near the pressure where it goes to zero. We note that at q values other than zero, this band shows little tendency to condense to zero frequency. In addition, there does not exist a strong hybridization of the parent B_u and B_g bands. Specifically, near $q=0.7$ where Mirgorodsky *et al.* predict a soft mode in Si_3N_4, we find no trend to soften. Thus our results indicate that the phase transition from $P6_3/m$ to $P\bar{6}$ (or $P3$) is driven by the Γ-point B_u phonon condensation, and it does not appear to give an commensurate structure, at least for large q (such as near 0.7). However, the frequency of the mode which at Γ is B_u is fairly flat near $q=0$, so we cannot rule out that some q values near zero (e.g., 0.0–0.2) does not become soft before the $q=0$ mode becomes soft. We are unable to explore this mode at pressures closer to the Γ-point softening pressure, since the finite displacement method produces uncertainty when the linear restoring force approaches zero.

IV. CONCLUSIONS

We have used LDA density-functional theory (GDFT) to investigate the electronic and vibrational properties of germanium nitride (Ge_3N_4). Both the hexagonal β phase and the cubic γ phase (with the spinel structure) have been studied in detail. The $\beta \rightarrow \gamma$ phase transition is predicted by theory at about 4–8 GPa, where experimental observed upper limit is about 12 GPa.

We find that electronically these are very interesting materials with band gaps in the optical region. We find (β, γ) phases to have gaps of (2.45, 2.17 eV) within the LDA, and (4.0, 4.0 eV) within the generalized density-functional theory (GDFT). The gaps are direct at Γ point, and similar to values for III nitrides like GaN. The GDFT correction is found to reorder of some conduction states, which we believe is the first example of this kind of behavior using GDFT.

The equations of state and internal coordinates have been computed. We have examined several possible candidate structures for the β phase under pressure, and find two changes of structure. The $P6_3/m$ ground-state structure under pressure changes to $P\bar{6}$, followed at higher pressure to $P3$. These transitions assume that the transition to the γ phase is suppressed by keeping the sample temperature at ambient.

The vibrational modes of β and γ phases have been evaluated and compared with experiment. All modes are identified and assigned to experimental peaks, and there is overall consistent agreement. The lowest T_{2g} mode for the γ phase has an anomalously large error however.

The pressure dependence of the modes for the β phase are studied and the Raman modes are compared favorably with experiment under 20 GPa. A silent B_u mode is found to become soft near 20 GPa, which is the origin of the $P6_3/m \rightarrow P\bar{6}$ phase transition encountered under metastable pressurization of β-Ge_3N_4. This transition is immediately followed (or is simultaneous with) a further reduction in symmetry to a $P3$ phase, which is now observed in experiments.[29,30]

ACKNOWLEDGMENTS

This work was supported by the NSF-ASU MRSEC (DMR-96-32635) on high-pressure materials synthesis. It is our pleasure to thank Michael O'Keeffe, Kurt Leinenweber, M. Somayazulu, and Herve Hubert for many insightful discussions that we had in the course of this work.

[1] R.N. Katz, Science **208**, 84 (1980).
[2] *Silicon Nitride in Electronics*, edited by V.I. Belyi *et al.*, Material Science Monographs Vol. 34 (Elsevier, New York, 1988).
[3] S. Wild, P. Grieveson, and K.H. Jack, Spec. Ceram. **5**, 385 (1972).
[4] B. Grün, Acta Crystallogr., Sect. B: Struct. Crystallogr. Cryst. Chem. **35**, 800 (1979).
[5] N. Wada, S.A. Solin, J. Wong, and S. Prochazka, J. Non-Cryst. Solids **43**, 7 (1981).
[6] K. Honda, S. Yokoyama, and S. Tanaka, J. Appl. Phys. **85**, 7380 (1999).
[7] S.Y. Ren and W.Y. Ching, Phys. Rev. B **23**, 5454 (1981); Y.N. Xu and W.Y. Ching, *ibid.* **51**, 17 379 (1995).
[8] A.Y. Liu and M.L. Cohen, Phys. Rev. B **41**, 10 727 (1990).
[9] J. Dong and O.F. Sankey, J. Appl. Phys. **87**, 958 (2000)..
[10] A.Y. Liu and M.L. Cohen, Science **245**, 841 (1989).
[11] D.M. Teter and R.J. Hemley, Science **271**, 53 (1996).
[12] J. Ortega and O.F. Sankey, Phys. Rev. B **51**, 2624 (1995).
[13] A.Y. Liu and R.M. Wentzocovitch, Phys. Rev. B **50**, 10 362 (1994).
[14] G. Serghiou, G. Miehe, O. Tschauner, A. Zerr, and R. Boehler, J. Chem. Phys. **111**, 4659 (1999).
[15] K. Leinenweber, M. O'Keeffe, M.S. Somayazulu, H. Hubert, P.F. McMillan, and G.H. Wolf, Chem.-Eur. J. **5**, 3076 (1999).
[16] M.S. Somayazulu, K. Leinenweber, H. Hubert, P.F. McMillan, and G.H. Wolf (unpublished).
[17] A. Zerr, G. Miehe, G. Serghiou, M. Schwarz, E. Kroke, R. Riedel, H. Fueb, P. Kroll, and, R. Boehler, Nature (London) **400**, 340 (1999).
[18] G. Kresse and J. Furthmüller, Comput. Mater. Sci. **6**, 15 (1996); G. Kresse and J. Hafner, Phys. Rev. B **47**, 558 (1993); G. Kresse and J.J. Furthmüller *ibid.* **54**, 11 169 (1996).
[19] D. Vanderbilt, Phys. Rev. B **41**, 7892 (1990); K. Laasonen, R. Car, C. Lee, and D. Vanderbilt, *ibid.* **43**, 6796 (1991); K. Laasonen, A. Pasquarello, R. Car, C. Lee, and D. Vanderbilt, *ibid.* **47**, 10 142 (1993); G. Kresse and J. Hafner, Phys. Rev. B **48**, 13 115 (1993); J. Phys.: Condens. Matter **6**, 8245 (1994).
[20] D.M. Ceperley and B.J. Alder, Phys. Rev. Lett. **45**, 566 (1980).
[21] J.P. Perdew, *Electron Structure of Solids '91*, edited by P. Ziesche and H. Eschrig (Akademie Verlag, Berlin, 1991), p. 11.
[22] K. Kohatsu and J.W. McCauley, Mater. Res. Bull. **9**, 917 (1974); K. Kato, Z. Inoue, K. Kijima, T. Yamane, and J. Kawasa, J. Am. Ceram. Soc. **58**, 90 (1975).

[23] Z.A. Weinberg and R.A. Pollak, Appl. Phys. Lett. **27**, 254 (1975); R. Karcher, L. Ley, and R.L. Johnson, Phys. Rev. B **30**, 1896 (1984); R.D. Carson and S.E. Schnatterly, *ibid.* **33**, 2432 (1986); A. Iqbal, W.B. Jackson, C.C. Tsai, J.W. Allen, and C.W. Bates, Jr., J. Appl. Phys. **61**, 2947 (1987).
[24] I. Chambouleyron and A.R. Zanatta, J. Appl. Phys. **84**, 1 (1998).
[25] L. Fritsche and Y.M. Gu, Phys. Rev. B **48**, 4250 (1993).
[26] L. Fritsche, Phys. Rev. B **33**, 3976 (1986); Physica B **172**, 7 (1991); J. Cordes and L. Fritsche, Z. Phys. D: At., Mol. Clusters **13**, 345 (1989); L. Fritsche, *Excited States and Electron-atom Scattering in Density Functional Theory*, edited by E.K.U. Gross and R.M. Dreizler (Plenum Press, New York, 1995).
[27] I.N. Remediaki and E. Kaxiras, Phys. Rev. B **59**, 5536 (1999).
[28] H. Hubert *et al.* (unpublished).
[29] G. Wolf *et al.* (unpublished).
[30] S.K. Deb *et al.* (unpublished).
[31] J. Dong, O.F. Sankey, and G. Kern, Phys. Rev. B **60**, 950 (1999).
[32] J. Dong and O.F. Sankey, J. Phys.: Condens. Matter **11**, 6129 (1999).
[33] S.K. Deb, J. Dong, H. Hubert, P.F. McMillan, and O.F. Sankey, Solid State Commun. (unpublished).
[34] A.P. Mirgorodsky, M.I. Baraton, and P. Quintard, Phys. Rev. B **48**, 13 326 (1993).